XLI CILAMCE
XLI Ibero-Latin American Congress on Computational Methods in Engineering
16-19 November, 2020 FOZ DO IGUAÇU PARANÁ - BRAZIL

Finite element analysis of cellular beam by load control method

L. Madeira[1], G. S. Vieira[2], J. G. Ribeiro Neto[3], L. R. Cruvinel[2]

[1]*Dept. of Mechanical Sciences, University of Brasilia*
leonardo.santos@aluno.unb.br
Campus Darcy Ribeiro, Brasilia, Brazil
[2]*Dept. of Civil Engineering, University of Uberlandia*
Campus Santa Monica, Uberlandia/Minas Gerais, Brazil
gregorio.vieira@ufu.br, lucasrabelo.c@gmail.com
[3]*Dept. of Structural Engineering, Remy Consulting Engineers*
Burlington/Ontario, Canada
juliano@remyeng.com

Abstract. Cellular beams are of great interest due to their great flexural rigidity, high section modulus, excellent height/weight ratio, economical and eco-sustainable construction, possibility of services through the openings of the web and architectural aesthetic appearance. This study perform an approach to the processes of numerical implementation via Finite Elements Method in cellular beams evaluating their elastoplastic behavior with focus on the Vierendeel mechanism. The numerical model was calibrated against the experimental results of Warren [1] and a comparative study is carried out with respect to the physical properties of the steel, allowing to understand the advantages that high-strength steel can promote in this kind of structure.

Keywords: Cellular beams, Finite elements method, High-strength steel

1 Introduction

Cellular beams are generally made from hot rolled I sections, cut longitudinally according to the layout that makes it possible to detach them as two halves, move and weld them, forming a beam with a height higher than the original section, with a sequence of openings in the web (Fig. 1). It is also possible to use an expansion plate to further increase the height of the final part. The failure modes of a cellular beam structure, as well as castellated

(a) Computerized cut of the web. El-Sawy et al. [2]

(b) Re-assembly by welding. Sonck et al. [3]

Figure 1. Cell beam manufacturing process

beams Ellobody [4], can be initiated by shearing, bending, lateral torsional buckling, welded joints rupture and by web post-buckling modes. Panedpojaman et al. [5] says the Vierendeel mechanism is the dominant failure mode in

beams with openings. The transfer of vertical shear force across the web opening can cause local bending moment, named as the Vierendeel bending moment which is the root cause of failure. The Vierendeel failure is defined as the continuous formation of plastic hinges at the ends of four T-sections above and below the opening under the combination of Vierendeel bending moment, local axial force and local shear force, as shown in the Fig. 2.

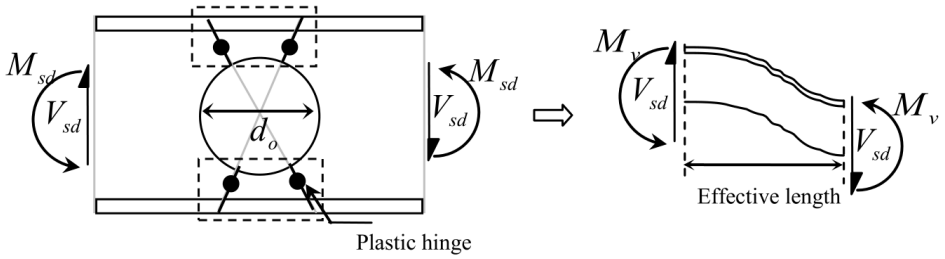

Figure 2. Vierendeel failure: plastic hinges and Vierendeel bending. Panedpojaman et al. [5]

As stated per Tsavdaridis and D'Mello [6], the Vierendeel mechanism is affected not only by the size of the opening, but also by its shape. The observation of formations of plastic hinges, followed by the redistribution of stresses along the opening can contribute to achieving greater loading capacities in steel beams with openings in the web. The cuts on cellular beams result in circular openings in the profile web. Following a similar principle, there are also the castellated beams, which are obtained with a cut that results in hexagonal openings. The cutting of the castellated beams can be carried out following some layout patterns. The most common are the Litzka, Anglo-Saxon and Peiner patterns.

According to Warren [1] cellular beams generally allow for larger spans concerning beams with full webs, for the same steel consumption. When cutting the beam, a beam with the same total mass is obtained, but more rigid than a beam with full web, due to the increase in the moment of inertia in the main plane of flexion. It is also possible to use openings for the passage of large diameter pipes and ducts, which makes cellular beams very versatile. The use of cellular beams occurs in situations in which it is necessary to overcome large spans, such as roofs of supermarkets or large stores, roof beams, floors of road and railway stations, roofs of industrial warehouses in frames and garage buildings. They are also used in roadway bridges or viaducts in which the openings in the beam's web are used for access to services, inspections, and maintenance. Another example of use can be found in the aerospace industry, being common the opening in the wings and fuselages of airplanes for passage of ducts, electrical wires, and cooling systems.

Veríssimo et al. [7] reports that one of the difficulties in working with cellular beams is due to the complexity in design, as each of the sections will be subject to a certain bending moment value and shear force. At first, it is not possible to determine which cross-section of the beam will result in the most unfavorable combination of forces, since the critical section does not always coincide with the maximum bending moment section, as usually occurs with full web beams. In these full web beams, it is also not usual to consider the portion referring to deformations from the shear force in the calculation of displacements. However, the deformations resulting from the shear stress can present an appreciable magnitude for the cellular beams, and should not be ignored.

According to Dowling [8] the plastic strain is caused by the change in the position of the atoms and their return to a stable state in a new configuration in your neighborhood after dislocation, being different from the elastic strain that is only the stretching of chemical bonds. Elastic strain occurs independently of plastic strain, when they occur simultaneously. If a yield stress is removed, the elastic strain is recovered as if it had not happened, but the plastic strain is permanent. In accordance with Santos [9], based on the different force levels achieved for high strength materials and ordinary materials, it is reasonable to conclude that a considerable reduction in the cost of the foundations of a multi-floor building is achieved with the use of high-strength materials adopted for the structure of the building. Therefore, the resistance of the materials must be taken into account when evaluating the use and costs involved in the execution of the structure. In addition, an economy of material and less socio-environmental impact are added to the construction with the use of high strength material.

2 Materials and methods

This section describes the problem and the methods used to resolve it. The adopted geometry is shown at Fig. 3(a). The validation results of the numerical model refer to point V3, as shown in the Fig. 3(b). The material properties are different for the flanges and the beam web, as Warren [1]. The yield stresses of the validated model

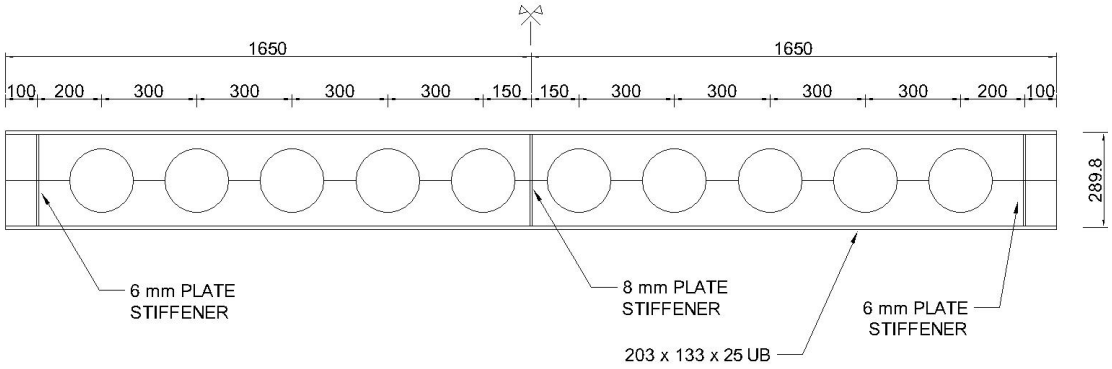

(a) Geometry problem

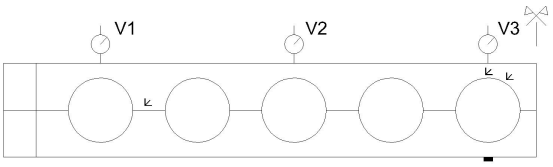

(b) Deflectometer positions

Figure 3. Reference experimental model. Warren [1]

are 297MPa and 279MPa for the web and flange, respectively. In comparison with high-strength steel (S460), the model given in RP-C208 [10] was used to find the true stress-strain relationship. Figure 4(a) shows the engineering stress-strain curves. All data used in the simulation are in terms of true stress-strain, as shown in Fig. 4(b). The expressions $\sigma^t = \sigma^e(1+\varepsilon^e)$ and $\varepsilon^t = ln(1+\varepsilon^e)$ were used for the conversion between engineering and true stresses/strains, agreeing with RP-C208 [10]. The material behavior is isotropic for the elastic and hardening phases.

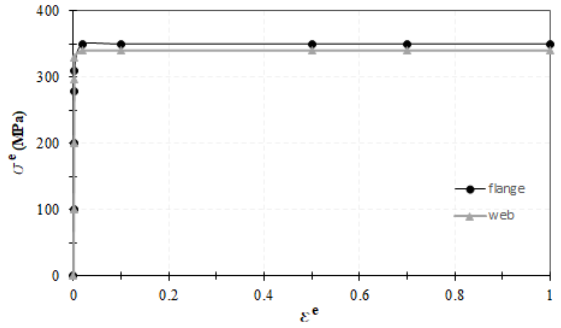

(a) Curve stress-strain (eng) Warren [1].

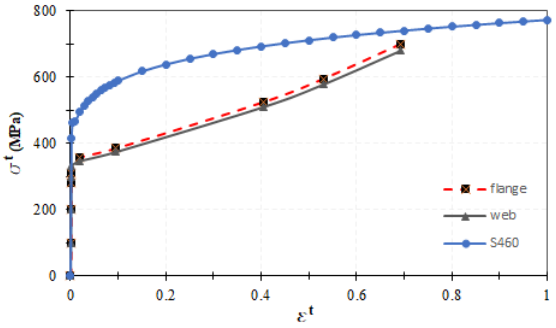

(b) Curve stress-strain (true)

Figure 4. Stress-strain diagrams for steels

This study was developed using the Abaqus 2017 software and the constitutive relations of von Mises were considered in the analysis, which is a model frequently used for steel elements. The numerical model consists in the same beam that was analysed by Warren [1] as simple supported beam with a concentrated load applied at the midle span. The concentrated load was implemented through the kinematic coupling constraint, in which all translations and rotations are restricted by coupling with a radius of influence to the most extreme point of the implementation region (Fig. 5). The stiffeners were linked to the beam web and flanges through the constraint Tie, where the stiffeners' contact region with the beam was considered to be a slave surface type, with the resulting master surfaces being the surfaces in the beam contact regions. A load of $130kN$ was applied at the reference point, which is applied uniformly to the beam surface by means of kinematic coupling restriction. The boundary conditions, as seen in Fig. 6, represent the supported configuration with $U1 = U2 = U3 = 0$ at one end and $U1 = U2 = 0$ at the other end. In addition, a restriction against rotation in direction 3, *i.e.*, $UR3 = 0$, on the top flange was adopted to avoid lateral buckling with torsion. In the Fig. 7 is presented the lateral and perspective views of the studied beam. Also is detached a refining mesh region where is possible to see the

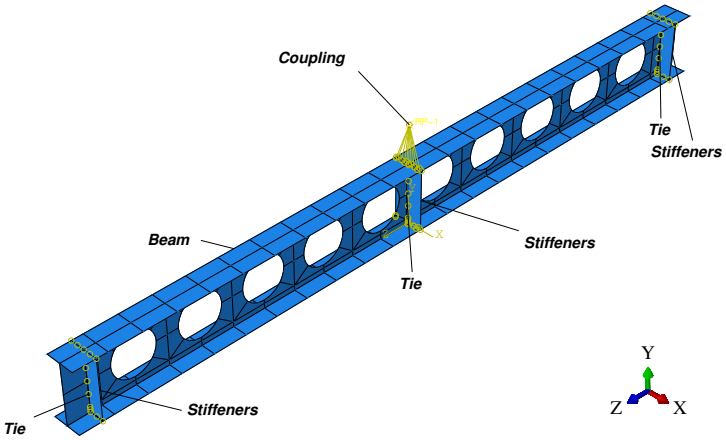

Figure 5. Constraints of the numerical model and assembly

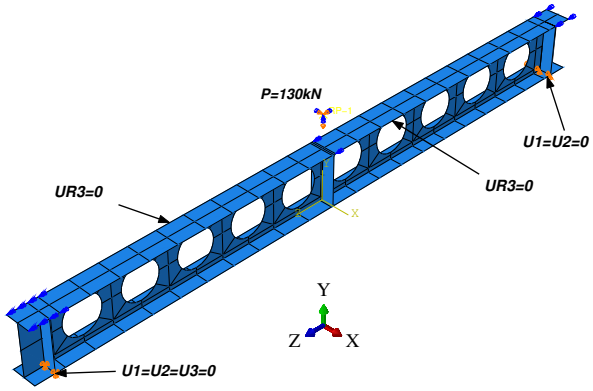

Figure 6. Loading and boundary conditions

transition areas (partitions) of meshing. That resource was implemented due to the curved format of the openings areas to possibility a smooth transition between the meshes. The three-dimensional numerical model has 9265 nodes and 8392 elements of the type $S4R$, which is a quadrilateral shell element with 4 nodes and 6 degrees of freedom per node, reduced integration with hourglass control and finite membrane strains. The numerical models

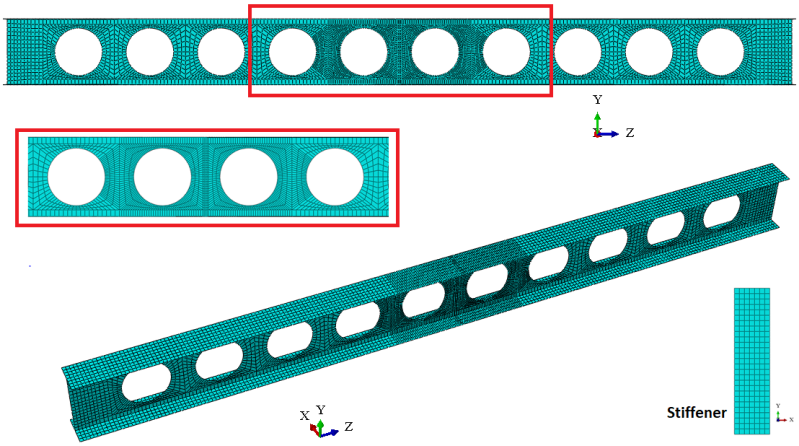

Figure 7. Mesh of the three-dimensional numerical model

were compared with experimental data in order to check how the differences between the load control application method and the displacement control method affect the computational response. In the models M-1 and M-2 are applied the load control and displacement control methods, respectively. For the purpose of comparing with other simulations, the results of the simulations via FEM of Warren [1] were also used as a calibration curve and model refinement.

3 Results and discussion

In the Fig. 8 is presented a curve force versus displacement to compare the numerical and experimental results. The numerical model M-1 is the closest behaviour to the experimental results. A greater difference is perceived in the elastic part of the force vs displacements curve, for the model in which displacement control was applied. However in the hardening part the numerical models show a results convergence and, the M-2 model is the closest to the experimental results, with little difference compared to the M-1 model. It is possible that the difference between experimental and numerical results can be reduced by implementing geometric imperfection. Also the stress concentrations in the welded region of the cell beam, if implemented, can contribute to the model refinement. As a comparisson, at the displacement of 9.8 mm the applied forces are 80 kN for the experimental result, 99 kN for M-1 and 102 kN for M-2 models. This represent a difference of 24% and 27%, respectively. In

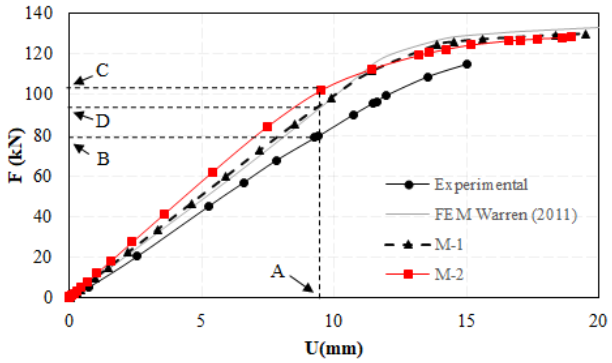

Figure 8. Curve force versus vertical displacement - model validation

the Fig. 9 is presented the displacements in the load application direction. The Vierendell mechanism is noticeable in the middle of the gap, due to a relevant change in the elastic line values, as can be seen in the middle of the openings near the middle span. This displacement is compatible with what is expected for the purpose of validating the numerical implementation, since there is a solidary displacement between stiffeners and the beam, with the displacement gradually increasing towards the middle of the span. The von Mises stresses, as expected,

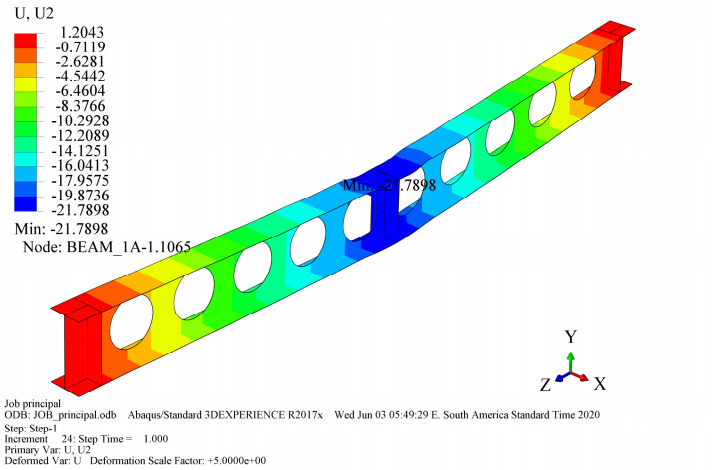

Figure 9. Vertical displacement, U2

have a gradient in the positions of greatest displacement, and have symmetry in relation to the central plane XY. The plastic deformation gradients are closer to the edges of openings in the path towards the middle of the span, as shown in the Fig. 11. The yield stresses are reached both in the web and in the beam flanges, with a failure in the flange and in the edge of the opening through the Vierendell mechanism, with plastic hinges at four points in the opening (Fig. 11 and Fig. 12(b)). In the Fig. 13 is presented the results of stress along the beam length. The path to the output was implemented in the beam symmetry region along the upper flange. For the numerical model with high-strength steel (M-3) the maximum stresses of $417.83MPa$ was reached at the coordinate of $1660mm$ along the span, as shown in the Fig. 13. This stress value exceeds the yield stress of $\sigma_{prop} = 414.8$ given in RP-C208 [10], however it is less than $\sigma_y = 462.8MPa$, where $\sigma_{prop} \approx 0.9\sigma_y$. It is also evident that in the center of the

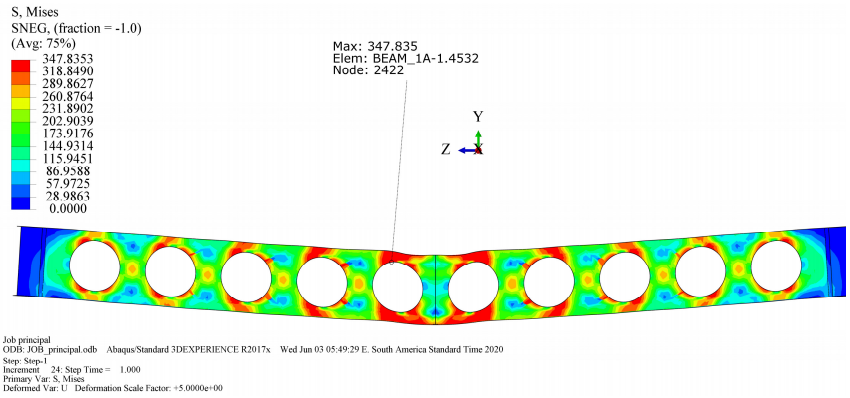

Figure 10. Von Mises stresses

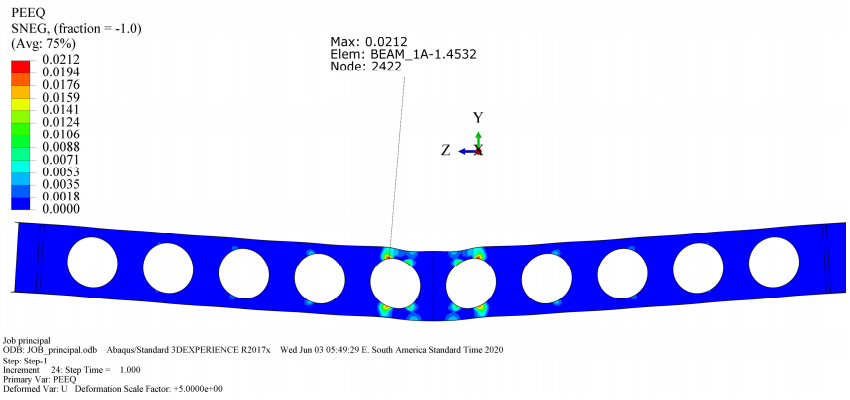

Figure 11. Equivalent plastic strain

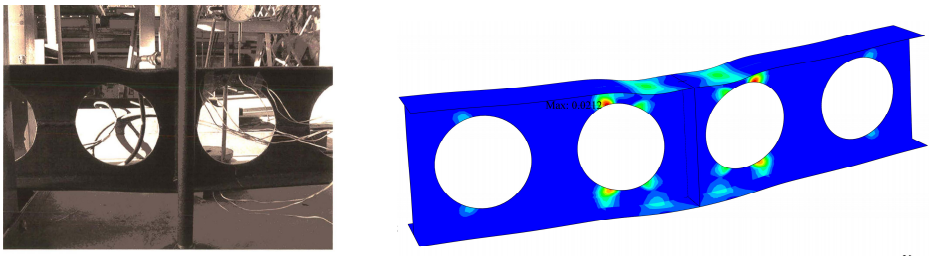

(a) Experimental test. Warren [1]. (b) FE model.

Figure 12. Vierendell mechanism in the central region of the cell beam.

holes there is a high-stress concentration in the flanges. This stress reduces along with the increase of web area until the region of full web, but restart to increase when appearing the next opening.

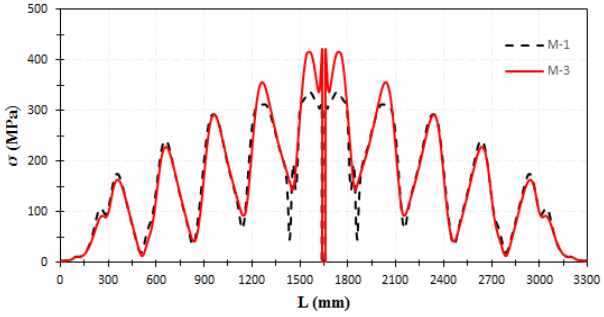

Figure 13. Von Mises stresses along the length of the upper flange

4 Conclusions

In this study, a numerical analysis was carried out via Finite Elements in a cell beam, validated with experimental results. Yield stresses and plastic strains are the main focus of the work, especially in the mid-span region and at the edge of the openings. The curve force versus vertical displacement between the numerical model and the experimental results showed a good correlation. Besides, that was also possible to see the stress variation along the beam and the Vierendell mechanism happening by the continuous formation of plastic hinges above and below the openings.

The implementation techniques were considered adequate, however, for a more detailed analysis it is necessary to insert the stress concentration phenomena due to the welds of the web. Based on the results obtained, it is concluded that the numerical model is representative of the experimental model and a viable and economical alternative for the structural analysis of cellular steel beams providing, even, a general analysis of all parts of the structure.

Acknowledgements. This work was partially supported by the Coordenação de Aperfeiçoamento de Pessoal de Nível Superior (CAPES) [Finance Code 001]. The authors gratefully acknowledge this support.

Authorship statement. The authors hereby confirm that they are the sole liable persons responsible for the authorship of this work, and that all material that has been herein included as part of the present paper is either the property (and authorship) of the authors, or has the permission of the owners to be included here.

References

[1] Warren, J., 2001. *Ultimate load and deflection behaviour of cellular beams*. Master's thesis, University of Natal, Durban.

[2] El-Sawy, K., Sweedan, A., & Martini, M., 2014. Moment gradient factor of cellular steel beams under inelastic flexure. *Journal of Constructional Steel Research*, vol. 98, pp. 20–34.

[3] Sonck, D., Van Impe, R., & Belis, J., 2014. Experimental investigation of residual stresses in steel cellular and castellated members. *Construction and Building Materials*, vol. 54, pp. 512–519.

[4] Ellobody, E., 2011. Interaction of buckling modes in castellated steel beams. *Journal of Constructional Steel Research*, vol. 67, n. 5, pp. 814 – 825.

[5] Panedpojaman, P., Thepchatri, T., & Limkatanyu, S., 2015. Novel simplified equations for vierendeel design of beams with (elongated) circular openings. *Journal of Constructional Steel Research*, vol. 112, pp. 10–21.

[6] Tsavdaridis, K. D. & D'Mello, C., 2012. Vierendeel bending study of perforated steel beams with various novel web opening shapes, through non-linear finite element analyses. *Journal of Structural Engineering*, vol. 138.

[7] Veríssimo, G. d. S., Vieira, W., Silveira, E., Ribeiro, J., Paes, J., Bezerra, E., Castro e Silva, A., & Fakury, R., 2012. Dimensionamento de vigas alveolares de aço. In *Congresso latino-americano da construção Metálica*.

[8] Dowling, N. E., 2013. *Mechanical Behavior of Materials: Engineering Methods for Deformation, Fracture, and Fatigue*. Pearson Education, 4 edition.

[9] Santos, L. M., 2019. *Análise numérica da interação mecânica de conector tipo pino com cabeça em vigas mistas*. Master's thesis, Faculty of technology - Department of mechanical sciences, University of Brasilia, Brasilia.

[10] RP-C208, D., 2016. *Determination of structural capacity by non-linear finite element analysis methods*. Det Norske Veritas & Germanischer Lloyd, Høvik.